Macromolecules

Article

pubs.acs.org/Macromolecules

# Wall Slip of Bidisperse Linear Polymer Melts

S. Mostafa Sabzevari,[†] Itai Cohen,[‡] and Paula M. Wood-Adams*[,†]

[†]Department of Mechanical and Industrial Engineering, Concordia University, Montreal, QC, Canada

[‡]Department of Physics, Cornell University, Ithaca, New York 14853, United States

**ABSTRACT:** We have characterized the effect of molecular weight distribution on slip of linear 1,4-polybutadiene samples sandwiched between cover glass and silicon wafer. Monodisperse polybutadiene samples with molecular weights in the range of 4−195 kg/mol and their binary mixtures were examined at steady state in planar Couette flow using tracer particle velocimetry. Slip velocity was measured at shear rates over the range of ∼0.1−15 $s^{-1}$. Our results revealed that weakly entangled short chains play a crucial role in wall slip and flow dynamics of linear polymer melts. It was found that the critical shear stress for the onset of the transition to the strong slip regime is significantly reduced when a small amount of weakly entangled chains is added to a sample of highly entangled polymer. Within the same range of shear stresses, binary mixtures of long and short chains exhibit significantly enhanced slip compared to the moderate slip of the individual long chains. This is attributed to the reduced friction coefficient at the polymer−solid interface which is likely a complicated function of the nature of entanglement, chain adsorption, and relaxation dynamics of chains at the interface.

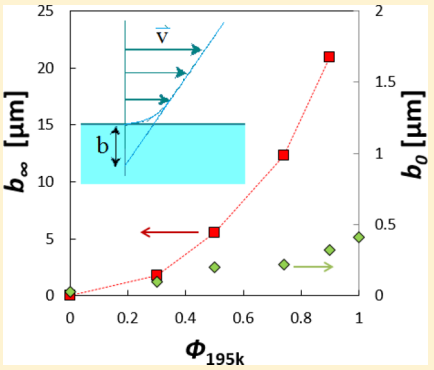


Historically, the no-slip liquid−solid boundary condition was presumed to be true for every type of problem in the field of fluid dynamics until implications of slip such as shear stress reduction, gap dependence shear stress, and flow rate discontinuity (spurt) showed up in the study of non-Newtonian fluids specifically polymers.[1] Today, it is well established that highly entangled linear polymer melts and concentrated solutions exhibit perceptible slip during flow on solid substrates.[2] Nevertheless, the extent to which polymers slip and its relationship to polymer structure still remains ambiguous due to the vast number of influential factors and the complexity of the phenomenon.[3,4]

Slip plays an important role in the flow dynamics of polymers in various practical applications such as extrusion, mixing, coating, and lubrication. Depending on the application, slip can be beneficial or detrimental. In polymer processing, slip is beneficial where (i) it reduces the required force/pressure for a certain drag/flow rate of fluid by lowering the wall shear stress and (ii) it (potentially) expands the margins within which defect-free and smooth-surface products can be produced (slip has been long related to surface distortions in extrusion-based polymer processing techniques although a clear cause−effect understanding has not yet been obtained).[4−16] Slip is detrimental (i) in polymer mixing where high shear is desired and (ii) in rheometry where accurate measurement of material properties requires ideal flow conditions. Therefore, the thorough characterization of slip is necessary not only to collect accurate rheological measurements but also to precisely design and produce polymers for particular applications such as lubricants, antislip polymers, and products with desirable surface finishes. Another important advantage of having this knowledge is that it allows for the development of accurate slip theories that can be used in flow simulations and other design analyses.

The factors influencing slip of polymers include the chemical and physical properties of both substrate and polymer: slip is most importantly affected by substrate surface energy, substrate roughness, polymer chemistry, molecular weight, molecular weight distribution, and chain architecture.[17−27] Although a great deal of knowledge has been well established on this subject—several comprehensive reviews can be found in refs 3, 4, and 21—the effects of parameters such as molecular weight distribution and low molecular weight chains have rarely been thoroughly explored in previous studies.[3,28] Polydispersity in molecular weight is a rather complicating factor in the field of polymer physics, and it has not yet been fully incorporated in polymer molecular theories even those for bulk rheology.[29] In the case of slip of polymers, the available molecular theories are applicable to monodisperse systems only and were never extended to polydisperse systems typical of industrial polymers.[30−35] In the most recent review of the subject in 2012 by Hatzikiriakos,[3] the author reminds us of the necessity of further work to investigate the effect of polydispersity on wall slip of polymers.

There is much experimental evidence that short chains or low molecular weight species play a critical role in physics and flow dynamics of molten polymers. Samples with broad molecular weight distributions are well-known to begin shear thinning at smaller shear rates compared to narrowly distributed samples. Several researchers[29,36−38] showed that

**Received:** February 27, 2014
**Revised:** April 9, 2014

   dx.doi.org/10.1021/ma500451g | *Macromolecules* XXXX, XXX, XXX−XXX

incorporation of short chains into the network of long chains accelerates relaxation of long chains and reduces the mixture plateau modulus, $G_N(\varphi)$. In capillary extrusion, Blyler and Hart[39] observed a considerable reduction in the magnitude of the flow curve discontinuity when different fractions of a low molecular weight polyethylene (PE) wax were added to a sample of high molecular weight linear PE. Similar results were found by Schreiber,[40] who also showed that the shape of molecular weight distribution influences the flow curve discontinuity and blends containing "components with widely different molecular weights are far more effective than broader but more normally shaped distributions" at reducing the magnitude of the discontinuity. Recently, Inn[16] studied capillary flow of three bimodal PE resins of similar viscosity. They observed that the sample with (i) higher content of the low molecular weight population and (ii) highest molecular weight of the high molecular weight population showed the largest slip as determined indirectly. These observations imply that short chains play a significant role in flow dynamics of highly entangled polymers. Here, we investigate slip of monodisperse and binary mixtures of polybutadiene (PBD) samples comprising long and short chains and varying "Struglinski–Graessley[37] parameter" $G_r$ where $G_r = M_2M_e^2/M_1^3$, $M_1$ and $M_2$ are molecular weights of short and long chains, respectively, and $M_e$ is the molecular weight between entanglements (for PBD $M_e$ = 1650 g/mol). The long chains in binary mixtures with $G_r > 1$ are known to exhibit constraint release in a dilated tube.[36−38,41] This indicates that the disentanglement believed to cause the onset of strong slip may be very different when $G_r > 1$. It would be interesting to examine the influence of short chains on slip of highly entangled polymers using a series of binary mixtures with $G_r > 1$.

In the present work, using tracer particle velocimetry in steady-state planar Couette flow, we report for the first time that a monodisperse sample of long chains exhibiting moderate slip undergoes substantial slip when mixed with a small fraction of weakly entangled short chains. These results can conveniently be exploited toward improving the existing slip theories. We also note that the use of planar Couette flow rules out the long-debated hypothesis of shear-induced fractionation which leads to the formation of a low-viscosity layer by migration of short chains toward the interface.[16]

## EXPERIMENTAL SECTION

We use narrow-distributed linear 1,4-polybutadiene (PBD) (cis 68%, trans 27%, and 1,2 addition 5%) with four different weight-average molecular weights: $M_w$ = 4, 73, 88, and 195 kg/mol and polydispersity indices PI ≤ 1.08 (Table 1) provided by Polymer Source Inc. Molecular weight distributions were measured using a Waters gel permeation chromatograph with tetrahydrofuran as diluent. The molecular weights are reported relative to polystyrene standards as determined from elution time and a refractive index detector.

**Table 1. Molecular Characteristics of Monodisperse PBDs**

| sym | $M_w$ [kg/mol] | $M_w/M_n$[a] | $M_w/M_e$ |
|---|---|---|---|
| 4K | 4.3 | 1.06 | 3 |
| 73K | 73.1 | 1.03 | 44 |
| 88K | 88.2 | 1.05 | 53 |
| 195K | 195.3 | 1.08 | 118 |

[a]$M_n$ is the number-average molecular weight.

All slip measurements were performed at room temperature. Experiments were carried out on monodisperse samples and their binary mixtures as shown in Table 2 ($\varphi_L$ is the weight fraction of long chains and $\eta_0$ is the zero shear viscosity). The Struglinski–Graessley parameters for the 4K/88K, 88K/195K, and 4K/195K binary mixtures are 3.023, 0.001, and 6.694, respectively.

**Table 2. Molecular Characteristics of Binary PBD Mixtures**

| sample | sym | $\varphi_L$ | $\eta_0$ [kPa·s] | $G_N$ [kPa] | $\tau_d$ [s] | $\sigma^*$ [kPa] |
|---|---|---|---|---|---|---|
| 4K/88K | B1 | 0.76 | NA[a] | NA[a] | NA[a] | NA[b] |
| 88K/195K | B2 | 0.51 | 21.5 | NA[a] | 0.03 | NA[b] |
| 4K/195K | L0 | 0 | 0.002[c] | NA[a] | NA[a] | NA[b] |
| 4K/195K | L30 | 0.30 | 0.9 | 73 | 0.03 | 2 |
| 4K/195K | L50 | 0.50 | 7.9 | 252 | 0.04 | 6 |
| 4K/195K | L74 | 0.74 | 27.0 | 502 | 0.07 | 20 |
| 4K/195K | L90 | 0.90 | 53.2 | 862 | 0.08 | 59 |
| 4K/195K | L100 | 1.00 | 71.7 | 1040 | 0.09 | 66 |

[a]LVE properties of this melt not measured due to instrument limitations. [b]Does not exhibit strong slip. [c]Obtained from ref 44.

To prepare binary samples, 5 wt % solutions of monodisperse PBDs in dichloromethane were mixed together in the appropriate proportions by weight to obtain the desired composition. A small amount (less than 0.5 wt %) of surface-treated (hexyltrimethoxysilane) fluorophore nanoparticles (nominal size of 75 nm) suspended in ethanol (2 mg/mL) was then added to each sample to be used as tracer particles for velocimetry measurements. Samples were dried at room temperature and under vacuum for 3 days to minimize residual traces of solvent molecules.

The dynamic linear viscoelastic properties were characterized by small-amplitude-oscillatory-shear (SAOS) measurements using a stress-controlled Paar Physica rotational rheometer (MCR 500). Measurements were done using 8 mm diameter stainless steel parallel plates with a gap of 1 mm under a nitrogen atmosphere. The plateau modulus $G_N(\varphi)$ was calculated from $G_N = 3.56G''_{max}$, which is an appropriate estimation for bidisperse samples of long and short chains as shown by Wang et al.[29] and Liu et al.[42] The disentanglement relaxation time $\tau_d$ was calculated from $\tau_d = 1/\omega_c$, where $\omega_c$ is the angular frequency at which $G'(\omega_c) = G''(\omega_c)$.[29]

Slip measurements were done by tracer particle velocimetry[2] utilizing a microfluidic shear cell and confocal microscopy. A detailed description of the experimental procedure can be found elsewhere.[2] The top plate was a silicon wafer whereas the bottom plate was a thin cover glass to transmit fluorescent light to, and from, nanoparticles. The gap was set to 85–90 $\mu$m, and the drag flow was provided by moving the bottom plate. During shearing, the polymer sample was illuminated by fluorescent light, and the reflection at the center of the sample and distance $z$ from the top plate was captured by a high-speed digital camera at 50 fps and with a 63× objective. Samples were sheared well into steady state as confirmed by the velocity–time data (see for example Figure 1) for all results presented here.

The velocity data including slip velocity and the corresponding shear rate in the steady-state region were then obtained through image processing using a modified version of MATPIV.[2,43] Confocal microscopy allowed us to observe the velocity profile across the gap.

The main quantity examined in this work is the slip velocity of PBD over the silicon wafer $v_s^t$ (which we refer to as $v_s$ hereafter). In order to locate the PBD–silicon wafer interface ($z$ = 0), the focal point of the objective was moved up toward the silicon wafer (stationary plate) until no tracer particles could be observed. The focal point was then slowly moved down (with increments of 0.1 $\mu$m) into the polymer sample until the very first tracer particles were observed. This point was regarded as $z$ = 0. This interface identification process was repeated three times to ensure the same location is inferred as the interface for each shear flow experiment. Considering the spatial resolution of the confocal microscope and the method we used to


dx.doi.org/10.1021/ma500451g | Macromolecules XXXX, XXX, XXX–XXX

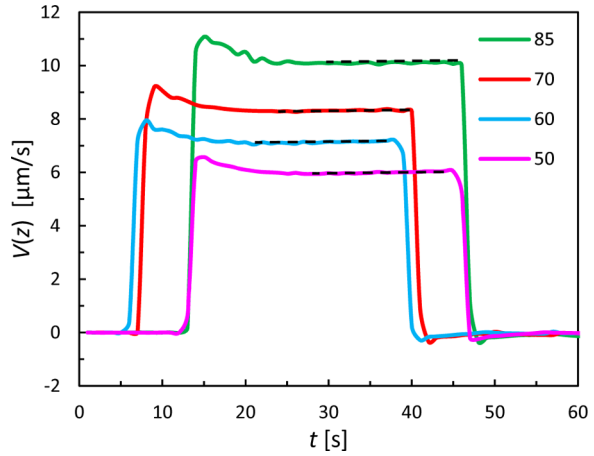


**Figure 1.** Velocity of nanoparticles $V(z)$ of binary sample L74 at different values of $z$ as labled (units are $\mu$m) as a function of time $t$. Steady-state velocity was ensured at long times. Dashed lines indicate steady-state values.

locate the interface, uncertainty in the location of polymer−solid interface as well as the slip length is ∼±0.1 $\mu$m.

The slip velocity at PBD−silicon wafer interface was measured over a wide range of nominal shear rates: $\dot{\gamma}_n \sim 0.1-15\ s^{-1}$. It is important to note that the maximum shear rate imposed on each sample is limited either geometrically or by the melt rupture of PBD at high shear stresses.

We performed additional measurements to examine the velocity profile across the gap at several rates. The profiles were found to be linear or slightly curved as shown for example in Figure 2. Since

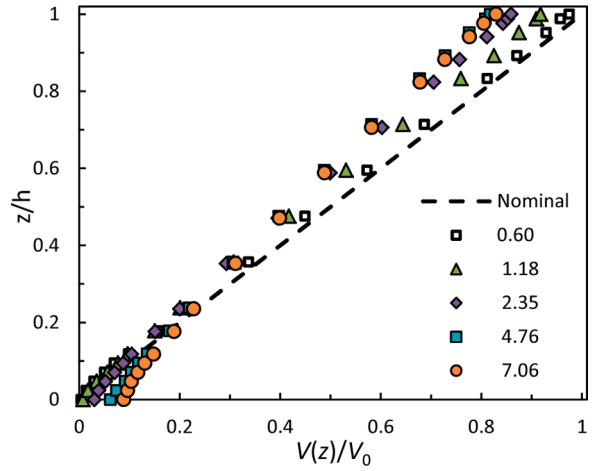


**Figure 2.** Normalized velocity profiles of binary sample L74 at nominal shear rates $\dot{\gamma}_n$ as labeled (units are $s^{-1}$). The vertical axis is the distance $z$ from the stationary plate (silicon wafer) normalized by the gap $h$ and the horizontal axis is the velocity of nanoparticles $V(z)$ normalized by the moving plate (cover glass, $z = 1$) velocity $V_0$.

obtaining the velocity profile requires a large amount of image processing, the velocity profile was measured only at five different rates on the order of ∼0.6, 1.2, 2.4, 4.8, and 7 $s^{-1}$ covering the entire range of weak to strong slip behavior.

Finally, we would like to consider the slip length $b$. The slip length is defined as the distance from the interface at which the velocity profile extrapolates to zero. In the planar Couette flow $b$ is defined as $b = v_s/\dot{\gamma}_T$ where $\dot{\gamma}_T$ is the true shear rate experienced by the sample: $\dot{\gamma}_T = \dot{\gamma}_n - (v_s^t + v_s^b)/h$. Here, $v_s^t$ and $v_s^b$ are slip velocities at the top (silicon wafer) and bottom (cover glass) plates, respectively, and $h$ is the gap between the two plates. We note that values of $v_s^t$ and $v_s^b$ are not the same. To calculate $\dot{\gamma}_T$ and hence $b$, we use the same $v_s^t$ based on direct measurement of slip velocity on silicon wafer. Since we measured the $v_s^b$ only at a few nominal shear rates (the same shear rates we did the velocity profile measurements), we estimate the rest of $v_s^b$ data through interpolation/extrapolation from those measured ($v_s^b$ versus $V_0$, see for example Figure 3).

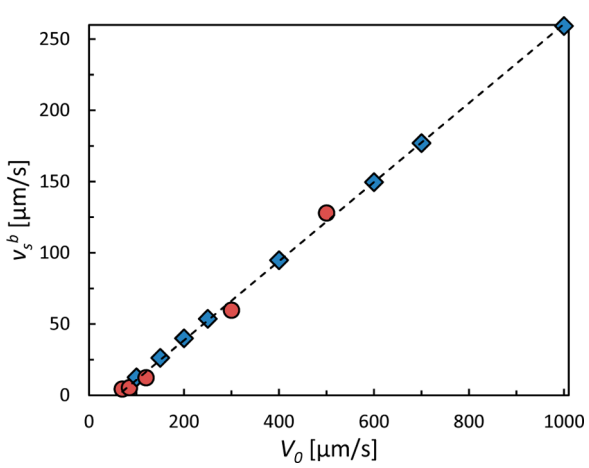


**Figure 3.** Slip velocity of L90 on cover glass $v_s^b$ versus moving plate velocity $V_0$. Solid circles are experimental data whereas solid diamonds are estimated data points by interpolation/extrapolation through linear regression (dashed line).

## RESULTS AND DISCUSSION

Understanding the wall slip of polymers requires knowledge of bulk rheological properties importantly viscosity in addition to near-wall properties. Figure 4 displays the rheological properties of binary 195K/4K PBD mixtures. As we will discuss in the upcoming sections, the systematic shift of the complex viscosity curve to lower values is a result of the simple dilution effect of short chains. This is important since it rules out the role of viscosity in any *abrupt* change in slip characteristics of binary samples as compared to the monodisperse constituents.

In the past, it was shown both experimentally[19,21,26] and theoretically[32,45] that slip of *highly entangled polymers* over solid substrates can be characterized by three distinct slip regimes: the weak slip regime, the transition regime, and the strong slip regime (known as macroscopic slip in capillary experiments).

The slip velocity as a function of shear stress $\sigma$ for the flow of monodisperse PBDs on silicon wafer is shown in Figure 5. The shear stress was calculated from $\sigma \cong \dot{\gamma}_T|\eta^*(\omega = \dot{\gamma}_T)|$, which is a realistic estimation since we use $\dot{\gamma}_T$ and we are close to the Newtonian plateau in all cases such that the Cox−Merz relation is very likely to be appropriate. For all samples (except the 4K chains) $\eta^*(\omega)$ was measured by SAOS using rotational rheometer. For the 4K chains, the Newtonian viscosity was taken from the literature.[44]

Several features can be understood from the data in Figure 5. Except for the high-shear stress portion of 195K, all monodisperse PBDs exhibit a power-low relationship between the slip velocity and shear stress: $v_s \propto \sigma^\alpha$ (here $\alpha$ varies from 0.74 to 1). Several previous researchers established similar relationships for the slip of linear polymers.[2,19,23] The 195K PBD sample exhibits different behavior: at high shear stresses, the slip transitions to a higher slip velocity regime (strong slip). For PBD, the strong slip regime has been observed for molecular weights above ∼100 kg/mol only.[9,24,46] Similarly,


dx.doi.org/10.1021/ma500451g | Macromolecules XXXX, XXX, XXX−XXX

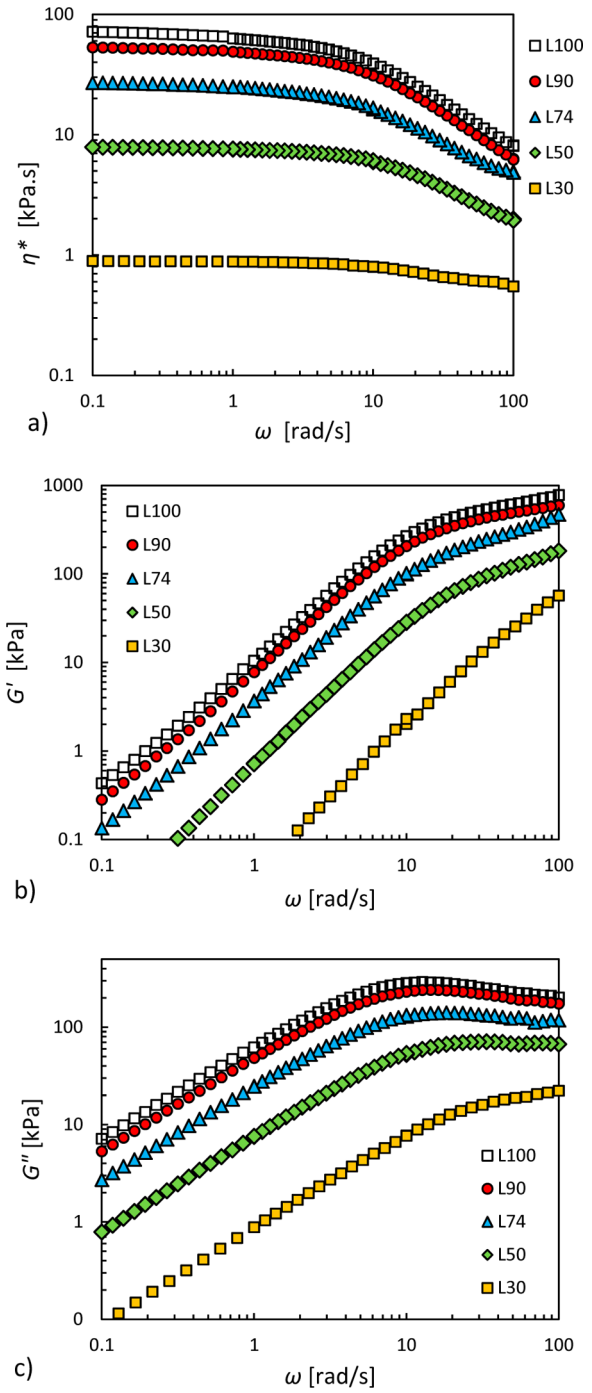


**Figure 4.** (a) Complex viscosity $\eta^*(\omega)$, (b) storage modulus $G'(\omega)$, and (c) loss modulus $G''(\omega)$ as a function of angular frequency $\omega$ of binary 4K/195K PBD mixtures.

Figure 5 confirms that PBD 195K is the only sample exhibiting a slight transition to the strong slip regime.

The data in Figure 5 as well illustrate another important feature; monodisperse PBDs with higher molecular weights require higher shear stresses to slip. For instance, 195K sample compared to 4K requires shear stresses orders of magnitude larger to exhibit the same slip velocity. This is an indication of a difference in the corresponding friction coefficient.

Brochard and de Gennes in their 1992 slip theory[33] introduced an alternative relationship for the shear stress under slip conditions: $\sigma = k_f v_s$ where $k_f$ is the friction coefficient

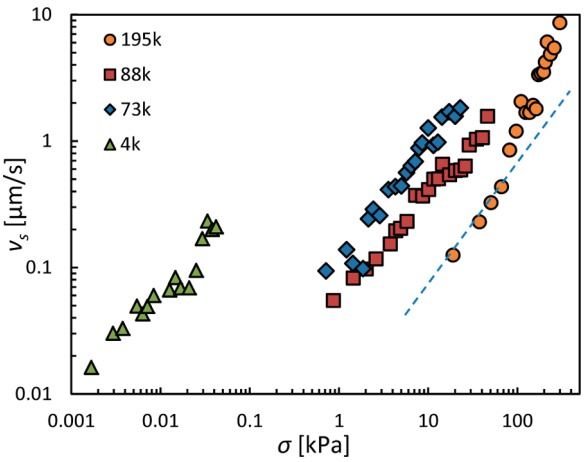


**Figure 5.** Slip velocity vs shear stress of monodisperse PBDs on silicon wafer. The dashed line is an extrapolation of the weak slip regime of the 195K sample to guide the reader's eye.

indicating the interactions between (i) the adsorbed and mobile chains (chain−chain interactions) and (ii) the mobile chains and wall (chain−wall interactions). Using the data in Figure 5, we calculate $k_f$ and plot it versus shear stress in Figure 6.

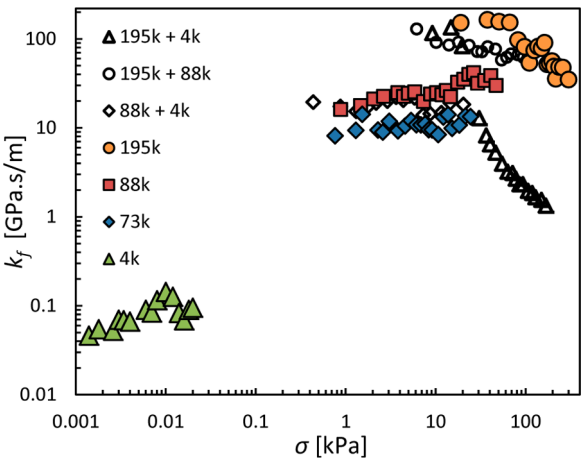


**Figure 6.** Friction coefficient vs stress of monodisperse PBDs (solid symbols) and their binary mixtures (open symbols) on silicon wafer.

Figure 6 shows the friction coefficient as a function of shear stress for monodisperse PBDs and selected binary samples on silicon wafer. For monodisperse PBDs, the friction coefficient at the weak slip regime $k_{f0}$ scales with the weight-average molecular weight as $k_{f0} \propto M_w^{2.1}$. This is in good agreement with the power of 1.5 that can be extracted using $k_{f0} = \eta_0/b_0$ from the work of Archer and co-workers[23] on monodisperse PBDs where they reported $b_0 \propto M_w^{1.94\pm0.07}$ and $\eta_0 \propto M_w^{3.4\pm0.02}$ ($b_0$ is the slip length at the weak slip regime).

To begin to understand the effect of polydispersity on slip, the first step is to investigate the slip of bidisperse mixtures. As seen in Figure 6, binary samples may exhibit significantly different behavior compared to monodisperse samples. Among three binary combinations of monodisperse 4K, 88K, and 195K PBDs, two of them 195K/88K and 88K/4K follow a close behavior to that of the long-chain constituent. The binary mixture of the longest and shortest chains (195K/4K: $G_r$ = 6.694) however exhibits a different behavior with the other two:


dx.doi.org/10.1021/ma500451g | Macromolecules XXXX, XXX, XXX−XXX

a very sharp transition toward much smaller values of friction coefficient.

Our first naïve impression from the results is that given sufficiently entangled long chains ($M_w/M_e$ > 118) to exhibit strong slip, the onset of the transition to the strong slip regime occurs much sooner once long chains are mixed with a sample of short-enough chains ($G_r$ > 1). Note that the binary sample 4K/88K with $G_r$ = 3.023 > 1 did not exhibit transition to strong slip simply because 88K chains are not entangled enough. We therefore examine the effect of long chain content of 195K/4K mixtures on their wall slip in the following.

The slip velocity as a function of the shear stress of 195K/4K binary mixtures on silicon wafer is shown in Figure 7 where slip

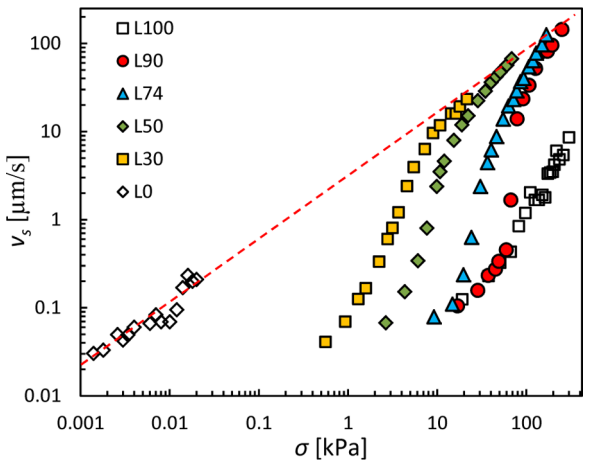


**Figure 7.** Slip velocity of binary 195K/4K PBDs (solid symbols) and their monodisperse constituents (open symbols) versus shear stress. The dashed line is an extrapolation of the slip of the 4K sample to guide the reader's eye.

curves of 195K and 4K, denoted by L100 and L0, respectively, were added to this graph for comparison. The results were striking; all binary samples exhibit a smooth transition from the weak slip regime to the strong slip regime where their slip velocity seem to follow the same trend as that of the short-chain component, i.e., 4K chains (once extrapolated). Compared to 195K chains, the binary mixtures exhibit strong slip at smaller shear stresses and they reach much higher slip velocities as well.

As seen in Figure 7, both the onset and slope of the transition regime change when a small amount of weakly entangled chains is added to a high molecular weight linear polymer. The slip curves of binary mixtures systematically vary with composition: the whole curve shifts to higher shear stresses and the transition to the strong slip regime becomes more *abrupt* as the content of long chains increases. In comparison, slip is suppressed in the case of the pure long chain sample. Moreover, the slip velocity of binary samples exhibits a smooth monotonic increase with stress in contrast to the increasing but rather erratic behavior of the monodisperse samples.

We start our analysis with investigating the effect of bidispersity on the value of the shear stress at the onset of the transition regime known as the critical shear stress $\sigma^*$. Several previous slip studies on heavily entangled polymer melts and solutions suggested that $\sigma^*$ which can be described as the critical shear stress required to disentangle adsorbed chains from the bulk is likely to scale with $G_N$ (a summary of these results can be found in refs 1, 23, and 24). No unique coefficient of proportionality can be established due to the large variation in different studies.

The data in Figure 7 show that in our case $\sigma^*$ varies with the content of the long chains in a systematic manner (we chose $\sigma^*$ of each binary mixture as the point right after which the slip curve branches off and the transition to higher slip velocities begin). Values of $\sigma^*$, $G_N$, and $\eta_0$ for binary and monodisperse constituents are listed in Table 2. Interestingly, $\sigma^*$ scales linearly with $\eta_0$, indicating a clear dependence of $\sigma^*$ on the weight-average molecular weight of binary samples. We note that this is likely because we are observing strong slip very close to the Newtonian plateau. Furthermore, we obtain $\sigma^* \propto G_N^{1.4}$ rather than the power of 1 found in the other studies. This relationship has not previously been characterized since we study binary mixtures instead of monodisperse samples.[24]

As mentioned previously, for PBD, the strong slip regime has been observed for molecular weights above ~100 kg/mol only. For binary mixtures composed of heavily and weakly entangled chains with $G_r$ > 1, the minimum degree of entanglement for strong slip reduces to about half of that of monodisperse samples: monodisperse PBD samples exhibit strong slip at $M$ > 100 kg/mol while a binary sample with $M_w$ as low as 62 kg/mol (L30) showed strong slip in this work. We note that Inn's[16] proposal that high content of small chains induces significant wall slip needs to be refined based on our results which clearly show that slip depends strongly on the chain length of both constituents.

Based on the Brochard–de Gennes' theory,[31,32] slip of highly entangled linear polymers can be explained by an entanglement–disentanglement mechanism between the moving and surface-adsorbed chains. The surface-adsorbed chains undergo a coil–stretch transition depending on the flow of the surrounding chains. According to this mechanism, in the weak slip regime at low slip velocities, the chains adsorbed on the wall are still entangled with the flowing chains and hence forced to comply with regulations of the bulk rheology. In the transition regime at intermediate velocities, the flowing chains start to undergo a repeating disentanglement–re-entanglement process with the adsorbed chains. In the strong slip regime at higher slip velocities, the moving chains become fully disentangled from the surface-adsorbed chains which consequently results in a friction coefficient similar to that of a flow of monomers.

Figure 8 displays the friction coefficient as a function of true shear rate for binary mixtures and their monodisperse constituents on silicon wafer. The use of shear rate instead of the shear stress on the horizontal axis allows us to study chain friction coefficient as a function of the rate of deformation. As can be seen in this figure, there is a fundamental difference between the behavior of friction coefficient in the weak and strong slip regimes denoted by $k_{f0}$ and $k_{f\infty}$, respectively.

At low shear rates, we can see the characteristic large entanglement-dominated friction factor which decreases by orders of magnitude as the average number of entanglements per chain is decreased with increasing low molecular weight chain content. Similarly to monodisperse PBDs, the $k_{f0}$ of binary mixtures scales with the weight-average molecular weight as $k_{f0} \propto M_w^{2.2}$, indicating that flow dynamics and interfacial properties of linear polymers at low deformation rates is mainly governed by their bulk rheology.

From the data in Figure 8, it is evident that the critical shear rate at the onset of the transition regime is almost the same as


dx.doi.org/10.1021/ma500451g | *Macromolecules* XXXX, XXX, XXX–XXX

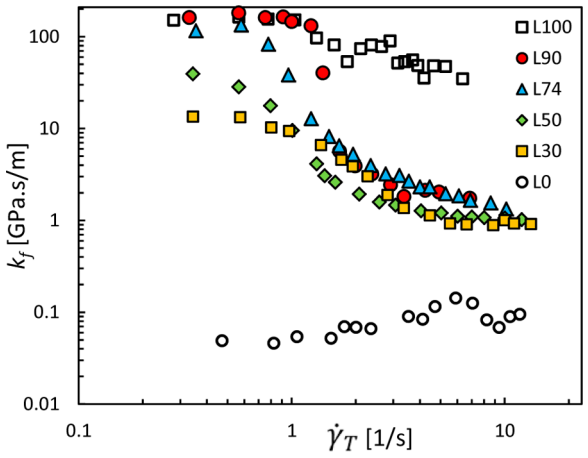


**Figure 8.** Friction coefficient versus true shear rate of binary 195K/4K PBDs (solid symbols) and their monodisperse constituents (open symbols).

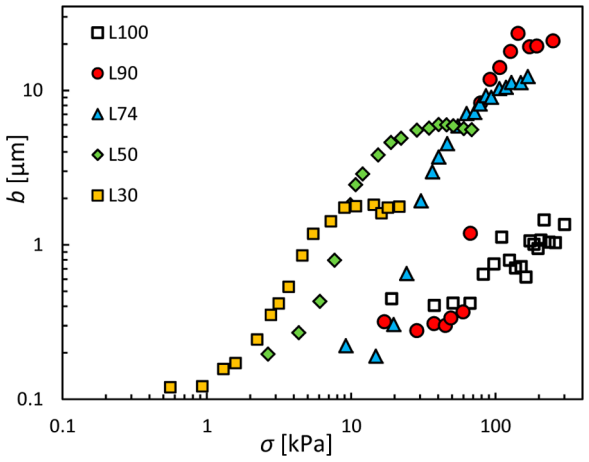


**Figure 9.** Slip length of binary 195K/4K PBDs versus shear stress.

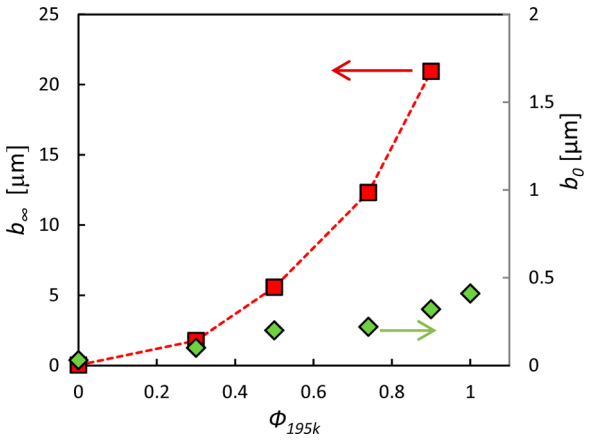


**Figure 10.** Slip length of binary 195K/4K PBDs versus weight fraction of 195K chains.

that of 195K: $\dot{\gamma}_T^* \sim 1\ s^{-1}$. This indicates that in binary mixtures it is the relaxation dynamics of the long-chain constituent that primarily governs the onset of the slip transition regime.

A very crucial outcome of this work is however the behavior of $k_{f\infty}$ of binary samples. As shown in Figure 8, the friction coefficient of all binary mixtures seems to be leveling off toward a plateau region. Under strong slip conditions, the mobile chains are disentangled from the chains adsorbed to the wall and the friction factor represents both unentangled chain−chain interactions and mobile chain−wall interactions. The fact that the pure L100 exhibits a higher $k_f$ than the binary mixtures indicates that one or both of these types of interactions is affected by the presence of the short chains. We recall that given the planar Couette flow conditions we do not expect any significant amount of shear-induced segregation of low molecular weight chains to the interface. Therefore, their presence at a concentration equal to that in the bulk is sufficient to cause a large increase in slip. It is important to note that we do not have enough data points to completely describe $k_{f\infty}$ of pure L100 since its $k_f$ seems to decrease further once we increase the deformation rate to higher values (not accessible with our current setup).

Slip length can also be described as $b = \eta/k_f$ where $\eta$ is the melt viscosity. This relationship states that slip length depends on both the friction coefficient and viscosity of the polymer and therefore cannot be an independent measure of the amount of slip. However, slip length can be a proper measure of the amount of viscous dissipation that a polymer sample undergoes during flow. In fact, it is the $b/h$ ratio ($h$ is the shear cell gap or tube diameter) that indicates how important the slip effects are at a macroscopic scale: $b/h \ll 1$ indicates negligible slip while $b/h > 1$ signifies considerable slip resulting in a velocity profile close to plug flow.

The slip length of binary 195K/4K PBD mixtures as a function of shear stress are shown in Figure 9. Similar to the behavior of monodisperse PBDs in the weak slip regime, $b_0$ of binary mixtures increases weakly with $M_w$ as a result of the increase in bulk viscosity. The slip length at the strong slip regime $b_\infty$ behaves differently since the $k_{f\infty}$ is drastically affected by the presence of short chains. The behavior of $b_0$ and $b_\infty$ as a function of $\varphi$ is shown in Figure 10.

As shown, for binary mixtures of long and short chains (195K/4K), $b_\infty$ shows a stronger dependence on $\varphi$ than $b_0$: $b_\infty \propto \varphi^{2.2}$ versus $b_0 \propto \varphi^{1.1}$. The difference between the power law dependence of $b_0$ and $b_\infty$ on $\varphi$ indicates that the presence of short chains in a binary mixture is more pronounced at higher stresses where mobile chains begin to disentangle from those adsorbed to the surface. The power law dependence of $b_\infty$ of binary mixtures on $\varphi$ is similar to that established between $G_N$ and $\varphi$ as $G_N \propto \varphi^{2.2}$.[29,37,38] The similarity between these parameters would be a promising starting point for further study of slip in polydisperse samples. It is important to note that $b_\infty$ of 195K may have not been reached within the range of shear stresses examined in this study, and hence it is not included in Figure 10. Sample L90 containing the highest content of long chains exhibited the most extreme slip with $b_\infty$ on order of 20 $\mu$m. The increase in $b_\infty$ of binary samples is most certainly due to a decrease in their corresponding friction coefficient as it is shown in Figure 8, signifying the important role of short chains in wall slip and flow dynamics of linear polymers.

## CONCLUSION

The results highlight the important role of weakly entangled chains in the course of polymer flow. Slip of binary mixtures of long and short chains with $G_r > 1$ in the strong slip regime is significantly affected by the presence of short chains. We showed that the addition of a small amount of short chains with $M \sim M_c \sim 3M_e$ to a monodisperse sample of sufficiently


dx.doi.org/10.1021/ma500451g | Macromolecules XXXX, XXX, XXX−XXX

entangled long chains $M \sim 118M_e$ significantly reduces the strong slip friction coefficient resulting in a significant increase in wall slip compared to moderate slip of long chains at the same shear stress.

Surprisingly, for binary mixtures the strong-regime slip length, $b_\infty$, scales with the content of long chains, $\varphi$, as $b_\infty \propto \varphi^{2.2}$, a relationship similar to that established between binary mixtures plateau modulus $G_N$ and $\varphi$ as $G_N \propto \varphi^{2.2}$. While the weak slip friction coefficient seems to scale well with bulk rheology and entanglement density of chains, the strong slip friction coefficient requires detailed knowledge of disentangled chain−chain and chain−wall interactions at the interface in addition to rheological properties. The lower stress decrease in $k_f$ of binary mixtures compared to monodisperse long chains indicates that the disentangled chain−chain and/or the chain−wall interactions at the interface are strongly affected by the presence of short chains.

We found that the critical shear stress $\sigma^*$ for the onset of transition to strong slip in binary PBD samples scales with $\eta_0$. We also showed that a binary sample with $M_w$ as low as 62 kg/mol could exhibit significant strong slip, although there exists specific requirements on the chain length of both of the individual constituents. In contrast, monodisperse samples with $M$ up to 195 kg/mol exhibited moderate slip only. These results provide the foundation for the development of new theoretical underpinnings for the mechanism by which short chains influence interfacial slip.

## AUTHOR INFORMATION


### Corresponding Author

*Tel (514) 848-2424-3815; e-mail paula.wood-adams@concordia.ca (P.M.W-A.).


### Notes

The authors declare no competing financial interest.

## ACKNOWLEDGMENTS

Wood-Adams was supported by an NSERC Discovery Grant and Concordia University. Cohen was supported in part by the US Department of Energy, Office of Basic Energy Sciences, Division of Materials Sciences and Engineering, under Award ER46517 and the National Science Foundation CBET-PMP Award 1232666. The authors gratefully acknowledge Neil Lin and Brian Leahy for their help in setting up the experimental apparatus.

## REFERENCES


(1) Archer, L. A. Wall Slip: Measurement and Modeling Issues. In *Polymer Processing Instabilities Control and Understanding*; Hatzikiriakos, S. G., Migler, K. B., Eds.; Marcel Dekker: New York, 2005.
(2) Hayes, K. A.; Buckley, M. R.; Cohen, I.; Archer, L. A. *Phys. Rev. Lett.* **2008**, *101*, 218301−4.
(3) Hatzikiriakos, S. G. *Prog. Polym. Sci.* **2012**, *37*, 624−643.
(4) Denn, M. M. *Annu. Rev. Fluid Mech.* **2001**, *33*, 265−287.
(5) Ghanta, V. G.; Riise, B. L.; Denn, M. M. *J. Rheol.* **1999**, *43*, 435−442.
(6) Kalika, D. S.; Denn, M. M. *J. Rheol.* **1987**, *31*, 815−834.
(7) Piau, J. M.; Kissi, N.; Mezghani, A. *J. Non-Newtonian Fluid Mech.* **1995**, *59*, 11−30.
(8) Ramamurthy, A. V. *J. Rheol.* **1986**, *30*, 337−357.
(9) Vinogradov, G. V.; Protasov, V. P.; Dreval, V. E. *Rheol. Acta* **1984**, *23*, 46−61.
(10) Wang, S. Q.; Drda, P. A. *Macromolecules* **1996**, *29*, 2627−2632.
(11) Wang, S. Q.; Drda, P. A. *Macromolecules* **1996**, *29*, 4115−4119.
(12) Wang, S. Q.; Drda, P. A. *Rheol. Acta* **1997**, *36*, 128−134.
(13) Yang, X.; et al. *Rheol. Acta* **1998**, *37*, 415−423.
(14) Yang, X.; et al. *Rheol. Acta* **1998**, *37*, 424−429.
(15) Kissi, N. El; Piau, J. M.; Toussaint, F. *J. Non-Newtonian Fluid Mech.* **1997**, *68*, 271−290.
(16) Inn, Y. W. *J. Rheol.* **2013**, *57*, 393−406.
(17) Archer, L. A.; Larson, R. G.; Chen, Y. L. *J. Fluid Mech.* **1995**, *301*, 133−151.
(18) Dao, T. T.; Archer, L. A. *Langmuir* **2002**, *18*, 2616−2624.
(19) Durliat, E.; Hervet, H.; Leger, L. *Europhys. Lett.* **1997**, *38*, 383−388.
(20) Hatzikiriakos, S. G.; Dealy, J. M. *J. Rheol.* **1991**, *35*, 497−523.
(21) Leger, L.; et al. *J. Phys.: Condens. Matter.* **1997**, *9*, 7719−7740.
(22) Legrand, F.; Piau, J. M.; Hervet, H. *J. Rheol.* **1998**, *42*, 1389−1402.
(23) Mhetar, V.; Archer, L. A. *Macromolecules* **1998**, *31*, 6639−6649.
(24) Mhetar, V.; Archer, L. A. *Macromolecules* **1998**, *31*, 8607−8616.
(25) Mhetar, V.; Archer, L. A. *Macromolecules* **1998**, *31*, 8617−8622.
(26) Migler, K. B.; Hervet, H.; Leger, L. *Phys. Rev. Lett.* **1993**, *70*, 287−290.
(27) Park, H. E.; et al. *J. Rheol.* **2008**, *52*, 1201−1239.
(28) Ansari, M.; et al. *J. Rheol.* **2013**, *57*, 927.
(29) Wang, S.; Wang, S. Q.; Halasa, A.; Hsu, W.-L. *Macromolecules* **2003**, *36*, 5355−5371.
(30) Ajdari, A.; et al. *Physica A* **1994**, *204*, 17−39.
(31) Brochard-Wyart, F.; de Gennes, P.-G.; Hervert, H.; Redon, C. *Langmuir* **1994**, *10*, 1566−1572.
(32) Brochard-Wyart, F.; Gay, C.; de Gennes, P.-G. *Macromolecules* **1996**, *29*, 377−382.
(33) Brochard-Wyart, F.; de Gennes, P.-G.; Pincus, P. A. *Acad. Sci.* **1992**, *314*, 873−878.
(34) Gay, C. *J. Phys. II* **1996**, *6*, 335−353.
(35) Gay, C. *Eur. Phys. J. B* **1999**, *7*, 251−262.
(36) Park, S. J.; Larson, R. G. *Macromolecules* **2004**, *37*, 597−604.
(37) Struglinski, M. J.; Graessley, W. W. *Macromolecules* **1985**, *18*, 2630−2642.
(38) Watanabe, H.; et al. *Macromolecules* **2004**, *37*, 6619−6631.
(39) Blyler, L. L.; Hart, A. C. *Polym. Eng. Sci.* **1970**, *10*, 193−203.
(40) Schreiber, H. P. *J. Polym. Sci., Part B: Polym. Lett.* **1969**, *7*, 851−860.
(41) Park, S. J.; Larson, R. G. *J. Rheol.* **2006**, *50*, 21−39.
(42) Liu, C.; et al. *Polymer* **2006**, *47*, 4461−4479.
(43) Hayes, K. A.; et al. *Macromolecules* **2010**, *43*, 4412−4417.
(44) Colby, R. H.; Fetters, L. J.; Graessley, W. W. *Macromolecules* **1987**, *20*, 2226−2237.
(45) Brochard, F.; de Gennes, P.-G. *Langmuir* **1992**, *8*, 3033−3037.
(46) Lim, F. J.; Schowalter, W. R. *J. Rheol.* **1989**, *33*, 1359−1382.